A Phase-Based Control Method to Control Power Flow of a Grid-Connected Solar Photovoltaics Through a Single Phase Micro-Inverter

Ferdian Ronilaya*, Ratna Ika Putri*, Mohammad Noor Hidayat*, Ahmad Hermawan*, Imron Ridzki*, Irham Fadlika**, Apripriharta‡**

*Department of Electrical Engineering, State Polytechnic of Malang, Jl. Soekarno-Hatta No. 9, 65141

**Department of Electrical Engineering, Faculty of Engineering, Universitas Negeri Malang, Jl. Semarang No. 5, 65145

(ferdian@polinema.ac.id, moh.noor@polinema.ac.id, ratna.ika@polinema.ac.id, ahmad.hermawan@polinema.ac.id, imron.ridzki@polinema.ac.id, irham.fadlika.ft@um.ac.id, apripriharta.ft@um.ac.id)

‡Corresponding Author: Apripriharta, Jalan Semarang No. 5 Malang 65145, Tel: +6282132580202, apripriharta.ft@um.ac.id,

Received: 20.04.2020 Accepted:29.05.2020

Abstract- This paper presents micro-inverter to regulate power delivery from a small scale solar photovoltaics using a phase-based control technique. The micro-inverter used is a flyback-type inverter. Instead of controlling the voltage magnitude, the proposed control method uses power angle as control parameter to yield maximum power. The phase angle is obtained from Maximum Power Point Tracker (MPPT) algorithm and then employed as the phase reference for shifting the power angle of sinusoidal signal from phase-locked loop (PLL) block. Several simulation experiments are performed to examine the design. A conventional technique is also presented for comparison. The simulated data shows that the implementation of this phase-based flyback inverter exhibits satisfactory results and hence can be used as an alternative method.

Keywords flyback-inverter, power angle, power flow, maximum power point tracker.

1. Introduction

Solar irradiance fluctuates violently and hence for an autonomous solar PV system, energy storage system is required to provide a stable power by mitigating transients. Energy storage is characterized by its short lifetime and costly. Unlike a stand-alone system, a grid connected solar PV uses grid networks as an infinite energy storage and provide cost advantages [1]. The concepts of micro-inverter, centralized systems and string-systems are the main technology used for solar PV systems connected to a grid network. Under partial shading conditions, the micro-inverter technologies provide improved performance compared with a centralized or string inverter [2]. Furthermore, it also provides benefits such as: lower installation cost, modular, ease of expandability and plug and play operation [3]. These features make it suitable for low power levels, typically for 150 – 300 W [4] and [5].

Some scholars have reviewed the micro-inverter technologies in [3 – 7], in which flyback-type inverter is the most attractive as it uses fewer components and simple controller. Moreover, it provides potentially low cost [8]. Generally, this inverter operates at DCM (discontinuous conduction mode) [9], [10]. For DCM operation, any change in input voltage will proportionally control the output current flow [9 – 12]. Thus, we can eliminate current sensor so that it can reduce costs. Power output of a micro inverter fluctuates sinusoidally with twice of the ac network frequency [13], [14]. But, this inverter input power is kept constant to maximize energy harvesting from the solar panel [15]. To overcome this power mismatch, the inverter needs a capacitor [16].

But, practically, a voltage ripple still exists in the primary side of the transformer. If this voltage ripple becomes higher, it can lead to current harmonics, and hence increases loss [17] and [18]. We can use a large electrolytic capacitor to solve such a problem. However, it may shorten the lifetime of the inverter [19] and [20]. To cope with this issue, Shimizu proposed a method so called power pulsation

decoupling method [21]. His method can reduce significantly the capacitance of DC input side of the inverter so that the ceramic or film capacitors can be used [22]. Nevertheless, the algorithm for additional decoupling circuit is complex. A simpler system is proposed by Zengin in [23]. His proposal is called "volt-second-based" technique. The main control parameter of the controller is voltage magnitude, in which the switch at dc side of the inverter is driven based on modulated "volt-second" product so as to the current envelope creates a pure sine wave. A control method that use signal's voltage in its operation has also been discussed by Han in [24]. By using a series-connected active buffer, this scheme can decrease the presence of second harmonic current. A dual-mode grid connected-flyback inverter has been proposed by Kim in [25]. The proposed method uses discontinuous conduction mode (DCM) and continuous conduction mode (CCM) operations. Repetitive control method is adopted to increase reference tracking accuracy. The main controller parameter used in this scheme is voltage signals.

A different approach is proposed in [26], [27] and [28], where current is used as a primary control parameter. Even though these controllers can achieve optimal power delivery goals, more power switches and magnetic devices are required and the control schemes are complex.

A feed-forward controller taking the capacitor current into account is proposed by Oscar in [29] and [30]. The aim of this study is to improve the power factor, particularly during light-load condition. The proposed method is done by using a synchronous rectifier circuit. Although high power factor in the light load can be obtained, we need additional power switches and hence increases cost.

A two-stage PV micro-inverter with adaptive inductor is discussed by Kan et al in [31]. The purpose of this adaptive inductor is to decrease the current stress of the inverter switches. Although this method can reduce the current stress of the power switches, the adaptive inductor may result in considerable additional losses.

The aforementioned methods use voltage and current signals as inverter control parameters. Instead of using the voltage and current as control parameters, this paper proposes a novel technique namely a phase based control method, in which it uses power angle as control parameter to yield maximum power. The phase angle is obtained from MPPT algorithm and then employed as a set value for shifting the sinusoidal wave phase from PLL block. Specifically, to the best authors' knowledge, there are no studies have been done to verify the effectiveness of this phase-based control method implemented in a flyback-type inverter.

The detailed analysis of flyback-type inverter is discussed in Section 2. Section 3 presents the proposed control of the inverter to regulate the power supplied to the low voltage ac network. The conventional design as proposed by Zengin in [23] is also discussed in this section. Simulation results and discussion are given in Section 4 and finally, Section 5 is conclusion.

2. Analysis of flyback-type inverter

Figure 1 shows a flyback-type inverter, in which it has one dc switch, Q1 and two ac switches, Q2 and Q3. To form AC voltage waveform, Q2 and Q3 work alternately with periods of 10 ms each for a grid frequency of 50 Hz. The passive filter used is an L-C-L type filter which is adopted from [32]

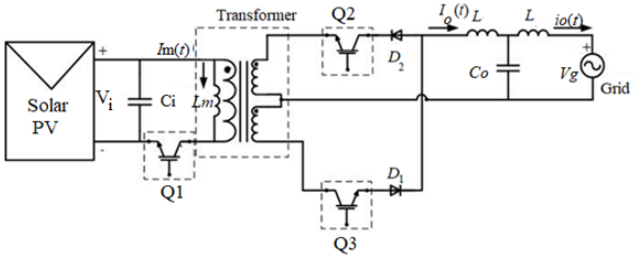

Fig 1. The circuit of flyback-type inverter [17].

When Q1 is turned on for ton second, current will flow to magnetizing inductance (Lm) and store the magnetic field energy. If Q1 is off for toff second, the stored energy in Lm is transferred to the ac network via D1 - Q3 (positive cycle) or D2 - Q2 (negative cycle). A discontinuous mode condition occurs when ton + toff is shorter than the switching of Q1, Tf. Thus, the maximum duty cycle, Dm, is expressed by the following equation:

$$D_m < \frac{NV_p}{NV_p + V_i} \tag{1}$$

where Vp is the maximum ac voltage grid, Vi is the inverter input voltage and N is transformer turn ratio. As this inverter operates in discontinous conducyion mode, the control of current is simply realized with no current sensor at ac side of the inverter [8] and [9]. But, we will get distorted output current when the inverter input voltage fluctuates. The energizing current, Im(t) increases linearly when Q1 is on and it can be expressed as follows:

$$\frac{v_i(t)}{L_m} = \frac{dI_m(t)}{dt} \tag{2}$$

with Lm represents the magnetizing inductance of transformer and its maximum current, Imp is given as follows (see Figure 2(a)):

$$I_{mp}(t) = \frac{v_i(t)}{L_m} \times t_{on}(t) \tag{3}$$

The relationship between duty cycle, d(t) and the sinusoidal reference waveform is given by Equation 4. In this case, the absolute sine wave is used as reference.

$$d(t) = Dm\,|\sin \omega t\,| \tag{4}$$

where Dm represents the maximum duty ratio. We can arrange the turn-on time equation as follows:

$$t_{on} = d(t) \times T_f \tag{5}$$

From Equation 3 and 5, the maximum current Imp becomes:

$$I_{mp}(t) = \frac{T_f d(t) v_i(t)}{L_m} \quad (6)$$

The magnetizing current will be transferred to the transformer secondary side when Q1 is off whose value is determined by the transformation rasio, N. Thus, the peak output current, Iop, is expressed by the following formula:

$$I_{op}(t) = \frac{N T_f v_i(t) d(t)}{L_m} \quad (7)$$

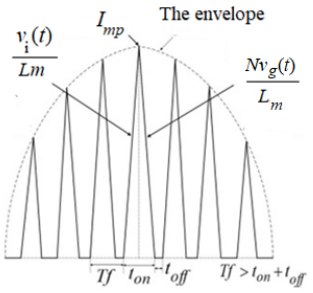

(a)

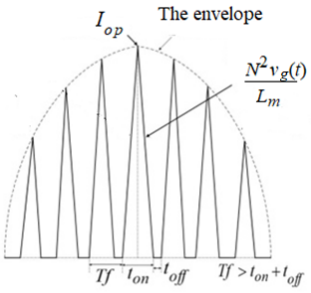

(b)

Fig. 2 (a). The current at dc side (b) The current at ac side during a first-half cycle.

The slope of output current is given by Equation 8.

$$\frac{dI_o(t)}{dt} = -\frac{N^2 V_g(t)}{L_m} \quad (8)$$

The voltage waveform of the grid is given by Equation 9.

$$v_g(t) = V_m \sin \omega t \quad (9)$$

where Vm represents the grid voltage amplitude. So, the time during off condition, toff, is shown by Equation 10.

$$t_{off}(t) = \frac{T_f v_i(t) d(t)}{N V_m \sin \omega t} \quad (10)$$

When we take the average value of a switching variable, this will cancel out the ripple caused by the IGBT (Q1, Q2 or Q3) switching process and hence allows modelling of low frequency fluctuations [23]. If we calculate the average value of the triangle waveform of the output current, then we will get the following equation:

$$i_o(t) = \frac{i_{op}(t) t_{off}(t)}{2T_f} \quad (11)$$

If Equation (7) and (10) are substituted into (11), we get:

$$i_o(t) = \frac{T_f V_i^2(t) d^2(t)}{2 V_m L_m \sin \omega t} \quad (12)$$

3. The controller design method

3.1 MPPT technique

The MPPT technique used in this study is Incremental Conductance (IC), in which the primary components include voltage and current sensors. The voltage and current of the solar PV is measured by these two sensors [33]. To mitigate the voltage and current ripple, we need low pass filter. In IC method, the output voltage is regulated such that the maximum power of solar PV is obtained. The basic operation of IC method is given by Figure 3(a) and the algorithm flowchart is shown by Figure 3(b).

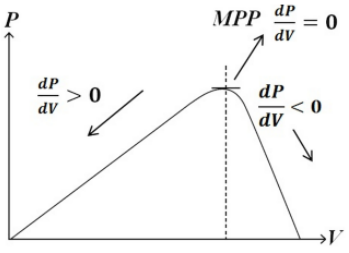

(a)

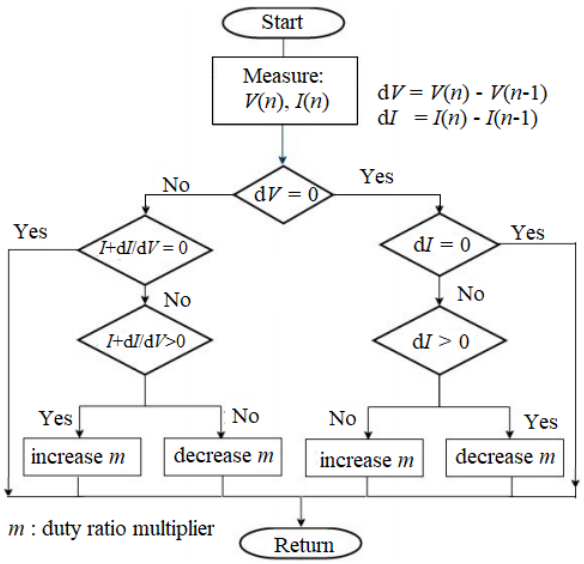

(b)

Fig. 3 (a). Basic operation of IC technique (b) the algorithm flowchart of IC method.

Figure 3(a) shows that the value of dp / dv equals zero when the solar PV operates at its maximum peak power (MPP). Figure 3(a) can be formulated by Equation 13 [34], [35]. V is the measured voltage of solar PV and I is solar PV output current. The left side of Equation 13 is incremental conductance whereas the right side of such equation represents the instantaneous conductance. This MPPT

algoithm is responsible for controlling the duty cycle multiplier ($m(t)$) so that it satisfies Equation 14 [36]. The implementation of this algorithm is given by a block diagram shown in Figure 4 [37].

$$\begin{aligned} &\frac{dI}{dV} = -\frac{I}{V} \text{ at MPP} \\ &\frac{dI}{dV} > -\frac{I}{V} \text{ at the left side of MPP} \\ &\frac{dI}{dV} < -\frac{I}{V} \text{ at the right side of MPP} \end{aligned} \quad (13)$$

$$\frac{dI}{dV} + \frac{I}{V} = 0 \quad (14)$$

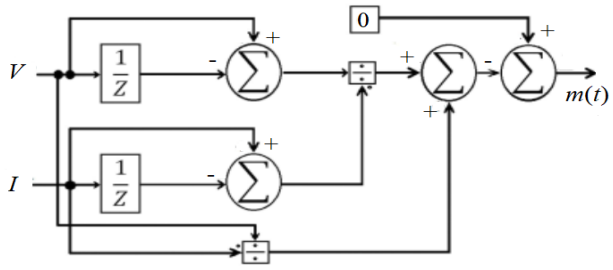

Fig. 4. The implementation of the IC MPPT method

3.2 The voltage-based controller

Equation 10 to 12 show that the output current supplied to the ac network is influenced by the duty cycle and the inverter input voltage. The input voltage of the inverter is kept constant and the duty cycle is modulated by using absolute value of reference sinusoidal wave (see Equation 4). In the this conventional controller, the duty cycle is regulated by varying the voltage magnitude. So, we can rearrange Equation 4 becomes:

$$d(t) = m(t) \times Dm \,|\sin \omega t| \quad (15)$$

where m(t) = output signal from MPPT, Dm = the maximum value of the duty cycle and ωt = the frequency signals from the PLL block to ensure the synchronism between the inverter output voltage and the grid. To get a better response, a PID controller is used. Thus, Equation 15 becomes:

$$d(t) = \mu(t) \times Dm \,|\sin \omega t| \quad (16)$$

where $\mu(t)$ is defined by the following equation:

$$\mu(t) = m(t)\left[G_p + G_i \int dt + G_d \frac{d}{dt}\right] \quad (17)$$

Gp = the proportional gain, Gi = the integral gain and Gd = the derivative gain. Then, $d(t)$ is used as a reference signal to generate a PWM signal for the power switch through a comparator. The control strategy of this concept is shown by Figure 5.

3.3 The phase-based controller

Instead of using the voltage magnitude as control parameter, the proposed method uses a phase difference between the ac network voltage (vg(t)) and the inverter output voltage (vo(t)) as the control parameter. Thus, Equation 4 is modified as shown by Equation 18.

$$d(t) = D_m \,|\sin \omega t \pm \delta(t)| \quad (18)$$

where δ (t) is power angle. It is the phase shift between the grid voltage and the inverter output voltage. From Equation 12 into 13, we can determine the output current of the inverter using the following equation:

$$i_o(t) = \frac{V_i^2(t) D_m^2 \sin^2(\omega t \pm \delta(t))}{2 f_s V_m L_m \sin \omega t} \quad (19)$$

The controller implementation of this concept is given by Figure 6.

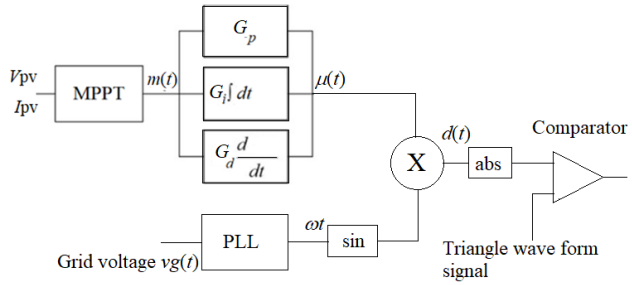

Fig. 5. The voltage-based controller

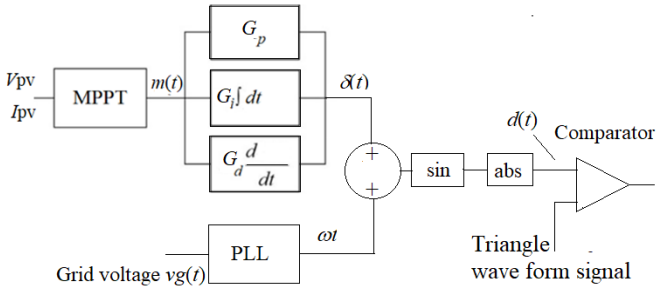

Fig. 6. The phase-based controller

4. Simulation results and discussion

The circuit of the phase-based controller is given by Figure 7 and Figure 8 shows the previous work so called a voltage-based controller as proposed by Zengin in [23]. To confirm the performance of the proposed method, several simulation experiments are carried out using Matlab software. The parameters of the investigated circuits are listed in Table 1. In the experimental simulation, the current of solar PV is measured by the dc current sensor. The switching frequency of Q1 is 8 kHz whereas Q2 and Q3 are switched alternately which are synchronized with the grid network. The inverter is operated in Discontinuous Conduction Mode.

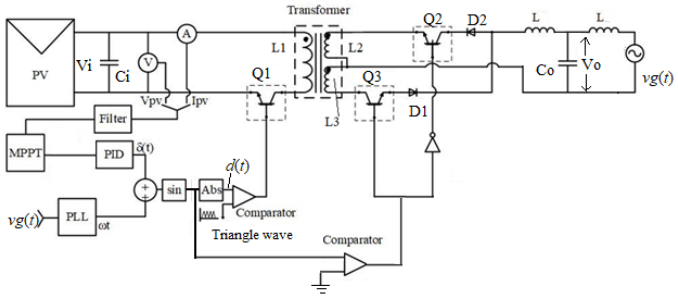

Fig. 7. The phase-based controller for flyback inverter

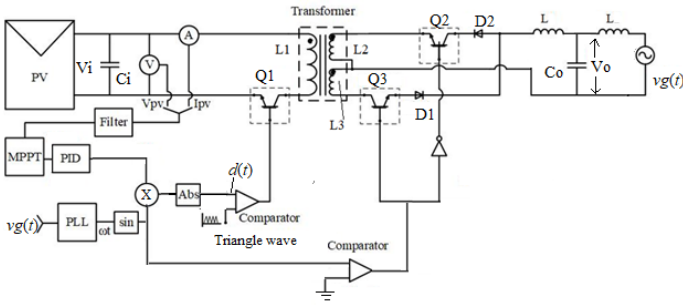

Fig. 8. The voltage-based controller for flyback inverter

Table 1. The parameters of the investigated circuits

Parameter	Value
Solar PV voltage	25 V
Grid voltage (rms)	220 V
Switching frequency	8 kHz
Solar PV Power	120 W
Grid frequency	50 Hz
Output inductor, L	4 mH
Output capacitor, C_o	3 µF
L_1, L_2, L_3	300 µH
Lm	400 µH
Turn rasio of the transformer, N	12
Input capacitance, C_i	3 mF

The inverter input voltage is shown by Figure 6 (a) and the input inverter current waveform is depicted by Figure 6 (b). It shows that the frequency of the waveforms is double that of the grid voltage because the sine voltage for the PWM system of Q1 has an absolute value that is in accordance with Equation 4 and 13.

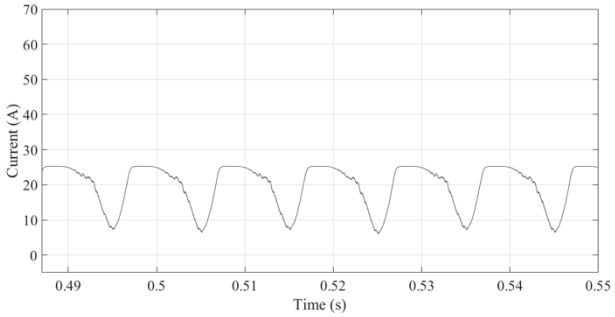

(a)

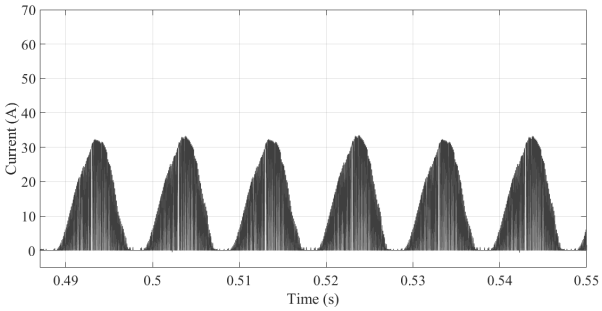

(b)

Fig. 6 (a) The voltage input waveform of the inverter (b) The current input waveform of the inverter

Figure 7 (a) and (b) show the output waveform of current and voltage when the inverter transfer power of 120 W with the input current and voltage of the inverter are kept constant. In this experiment, the value of solar irradiance used is 1000 W/m2 with a temperature of 25 oC.

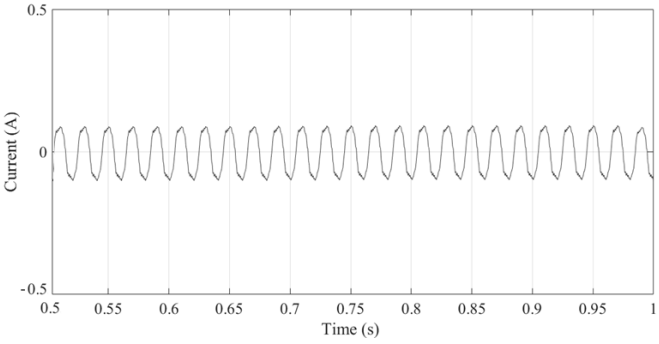

(a)

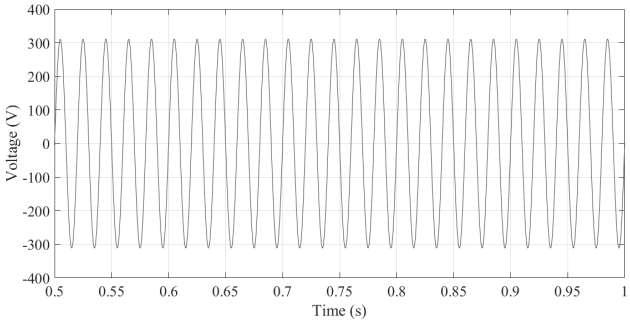

(b)

Fig. 7 (a) The current output (b) The voltage output

4.1 Power factor profiles

Solar PV is usually operated at a unity power factor. However, according to the standards recently discussed, each PV unit is permitted to participate in the contribution of reactive power to the grid to support voltage control. Fig. 8(a) and 8(b) show the voltage and current profiles under the phase-based controller and the voltage-based controller, respectively. In Figure 8 (a), the current lags behind the voltage so that the solar PV will send reactive power to the grid and contribute to the improvement of the power factor. On the other hand, Figure 8(b) shows that current and voltage are in phase and the inverter operates in a unity power factor. There is no reactive power delivered to the grid. It is assumed that the irradiace used is 1000 W/m^2.

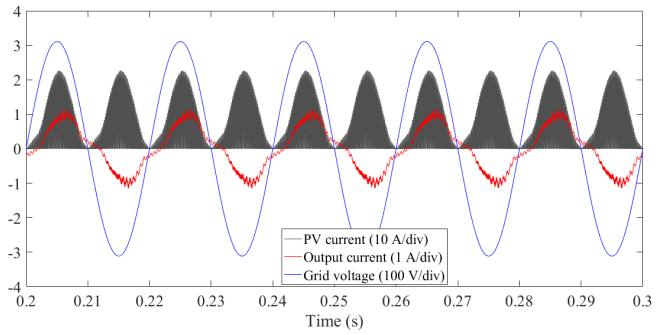

(a)

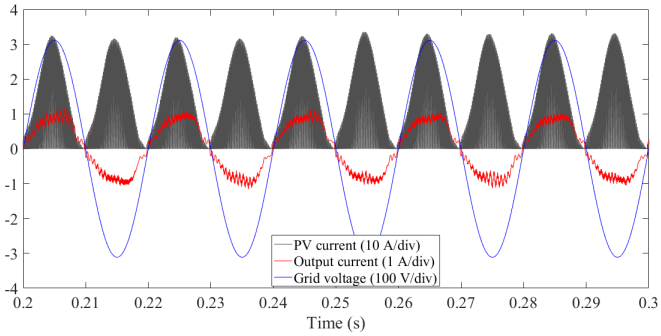

(b)

Fig. 8 (a). The voltage and current profiles under the proposed method. (b). The voltage and current profiles under the conventional method

Table 2 shows the power factor under various irradiance condition for both the proposed method and the conventional method as investigated by Zengin in [23]. Figure 9 shows the active and reactive power of each solar irradiance. On average, the reactive power supplied by the inverter using the conventional controller is zero. In contrast, the inverter that uses the phase-based controller is able to provide reactive power support to the grid and hence it may improve the power factor at the point where the solar PV is connected.

Table 2. The power factor measured at the grid.

Irradiance (W/m^2)	Power factor (%)	
	The proposed controller	The conventional controller
400	92.83	93.97
500	92.87	93.64
600	92.85	88.05
700	92.94	87.37
800	93.01	86.85
900	93.06	86.45
1000	93.10	86.41

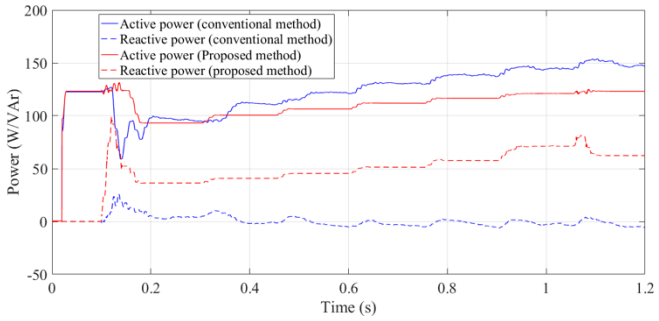

Fig. 9. Power responses under step changes of irradiance

4.2 Harmonic distortion

One of the main problems of the flyback inverter design is the existence of voltage riple whose frequency is twice the grid frequency. This voltage ripple can reduce the performance of the solar PV system, such as reducing MPPT performance and causing harmonics [22]. A simple way to overcome this problem is to use a dc-link capacitor. Table 3 shows the THD of the current for different capacitor values. The irradiance used is 1000 W/m^2. The harmonic spectrum under 1 mF capacitor is shown by Figure 10 whereas Figure 11 is the spectrum when the inverter uses a 6 mf capacitor.

Tabel 3. THD of current for both the proposed method and the conventional method

Ci	THD (%)	
	Proposed method	Conventional method
0.1 mF	20.55	31.1
0.5 mF	20.4	30.96
1 mF	20.42	18.33
2 mF	21.3	14.86
3 mF	21.91	16.36
4 mF	22.73	16.76
5 mf	22.75	48.57
6 mF	23.12	55.04

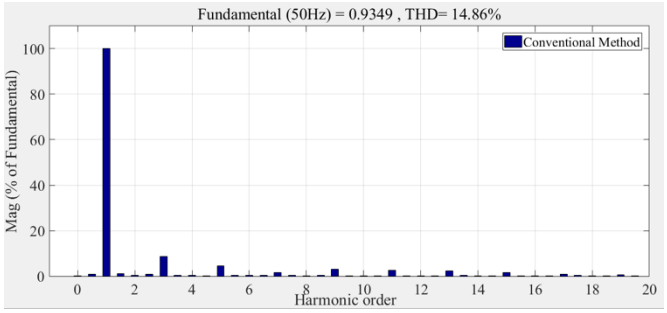

(a). Conventional method

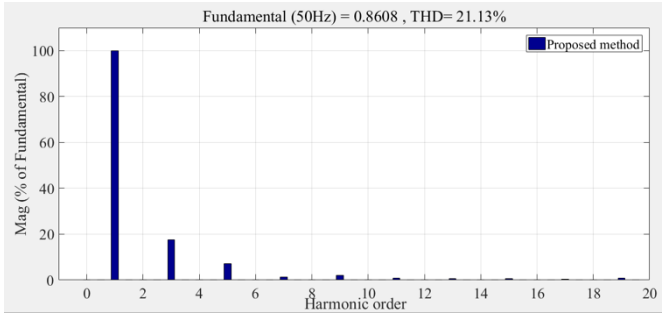

(b). Proposed method

Fig. 10. The frequency spectrum when Ci = 1 mF

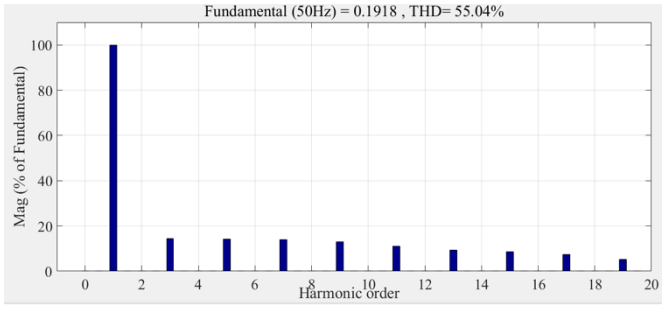

(a). Conventional method

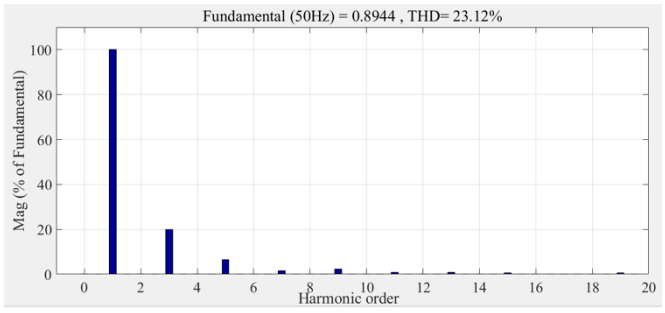

(b). Proposed method

Fig. 11. The frequency spectrum when Ci = 6 mF

For the proposed controller, we can see that the input capacitance value does not have much effect on the THD profile. Conversely, for the conventional controller, the input capacitance Ci is very influential on the THD level.

4.3 Power responses under fluctuating irradiance profile

The solar irradiance model shown in Figure 12 is used for examining the performance of the proposed approach. This model is adopted from Ref. [34].

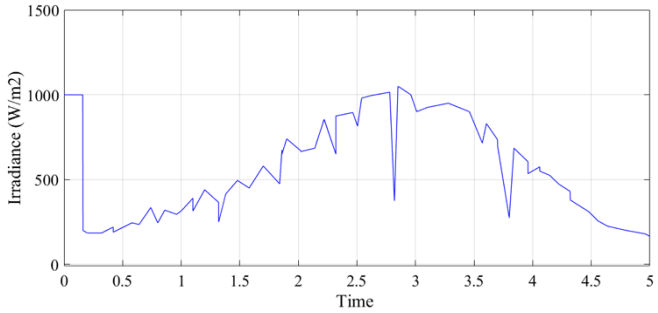

Fig. 12. The solar irradiance model

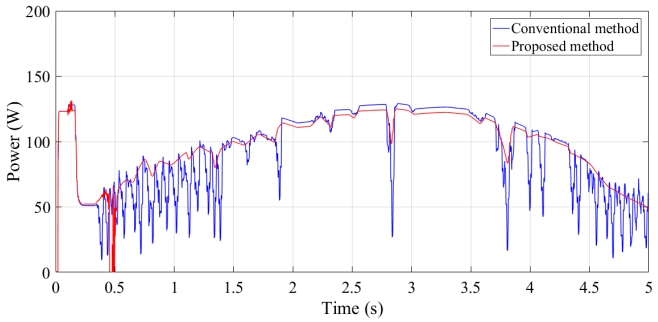

(a)

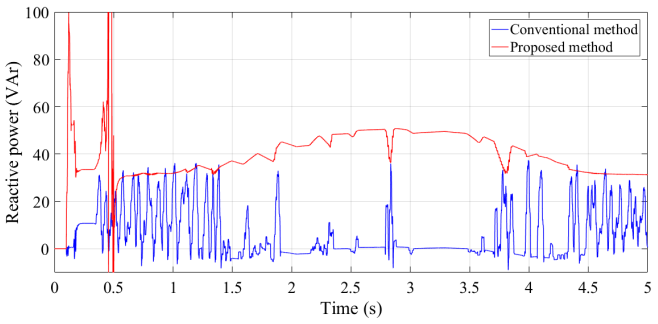

(b)

Fig. 13. (a) The active power responses. (b). The reactive power responses

The active power reponses for both the conventional and the proposed method is shown by Figure 13 (a). For low irradiance level, the conventional controller (blue line) exhibits oscillatory response. In contrary, the proposed controller delivers non-oscillatory active power (red line). Figure 13(b) depicts the reactive power responses for both the conventional and the proposed one. We can see that the conventional controller has oscillatory reactive power response and tend to have an average value of zero VAr. This is different from the proposed controller in which the system is able to provide reactive power to the grid with a non-oscillatory power response. Thus, the proposed controller can be used to improve power factor at the point where the grid-connected PV is connected.

5. Conclusion

A phase based control technique to get maximum power delivery of a grid connected solar PV has been discussed. The power is supplied to the grid via a flyback inverter which is controlled by a phase-based control method. To confirm the effectiveness of the design, a conventional method is also discussed for comparison. Several simulation experiments have been carried out and the results are compared with that the voltage based technique. When Ci = 1 mF, the THD current level for the conventional controller is 14.86 % and while the current THD level for the proposed controller is equal to 21.13 %. However, when Ci = 6 mF, the conventional controller gives a current THD value of 55% while the proposed controller gives a value of 23.12%. For the proposed controller, the input capacitance value does not have much effect on the THD profile. Conversely, for the conventional controller, the input capacitance Ci is very influential on the THD level. In term of power responses, the conventional controller hase oscillatory response. In contrary, the proposed controller delivers non-oscillatory power. Additionally, the conventional controller has oscillatory reactive power response and tend to have an average value of zero VAr. This is different from the proposed controller in which the system is able to provide reactive power to the grid with a non-oscillatory power responseso that it can be used to improve power factor at the point where the grid-connected solar PV is installed.

Acknowledgements

The authors would like to thank State Polytechnic of Malang and the Ministry of Education and Culture, Indonesia for their financial support in this work.

References

[1] S. Kirmani, M. Jamil, I. Akhtar, “Effective low cost Grid-Connected Solar Photovoltaic System to Electrify the Small Scale industry/Commercial Building”, in International Journal of Renewable Energy Research, vol. 7, No. 2, pp. 797 – 806, 2017

[2] H. Hu, S. Harb, N. Kutkut, I. Batarseh, Z. J. Shen. “Power decoupling techniques for micro- inverters in PV systems – a review”, En. Conv. Congress and Expo. (ECCE) pp 3235–3240, September 2010

[3] J. Yuan, F. Blaabjerg, Y. Yang, A. Sangwongwanich and Y. Shen, "An Overview of Photovoltaic Microinverters: Topology, Efficiency, and Reliability," 2019 IEEE 13th International Conference on Compatibility, Power Electronics and Power Engineering (CPE-POWERENG), Sonderborg, Denmark, pp. 1-6, 2019.

[4] J. M. Kwon, B. H. Kwon, K. H. Nam, “High-efficiency module-integrated photovoltaic power conditioning system,” IET Power Electron, vol 2 no 4 pp 410–420, 2009.

[5] S. B. Kjaer, J K Pedersen, F. Blaabjerg “A review of single-phasegrid-connected inverters for PV modules” IEEE Transac. Indus. Appl. vol 41 no 5 pp 1292–1306, 2005

[6] Q. Li, P. Wolfs, “A rev. of the single phase photovoltaic module integrated converter topologies with three different DC link configurations” IEEE Transac. Power Elec. vol 23 no 3 pp 1320–1333, 2008

[7] Y. Xue, L. Chang, S. B. Kjaer, J. Bordonau, T. Shimizu, “Topologies of single-phase inverters for small distributed power generators An overview” IEEE Transac. Power Electron. vol 19 no 5 pp 1305–1314, 2004

[8] Y. Li, R. Oruganti, “A low cost flyback CCM inverter for ac module application” IEEE Trans. Power Electron, vol 27 no 3 pp 1295–1303, 2012

[9] N. Kasa, T. Iida, L. Chen, “Flyback inverter controlled by sensorless current MPPT for photovoltaic power system”, IEEE Trans. Ind. Electron, vol 52 no 4 pp 1145–1152, 2005

[10] Y. Konishi, S. Chandhaket, K. Ogura, M. Nakaoka, “Utility-interactive high-frequency flyback transformer linked solar power conditioner for renewable energy utilizations" 4th Power Electronics and Drive Systems) vol 2 pp. 628–632, October 2001

[11] G. H. Tan, J. Y. Wang, Y. C. Ji, “Soft switching flyback inverter with enhanced power decoupling for photovoltaic applications” IET Electr. Pow. Appl vol 1 no 2 pp 264–274, 2007

[12] T. Brekken, C. Heme, L. R. Moumneh, N. Mohan “Utility-connected power conv. for maximizing power transfer from a photovoltaic source while drawing ripple-free current” Proceed. 33rd Annual Pow. Elect. Spec. Conf. vol 3 pp 1518–1522, 2002.

[13] Ertasgin, G.; Whaley, D.M.; Ertugrul, N.; Soong, W.L, “Analysis of DC Link Energy Storage for Single-Phase Grid-Connected PV Inverters”, vol. 8, No. 6, pp 1 – 19, 2019.

[14] M. H. Zare, M. Mohamadian and R. Beiranvand, "Single-stage AC module with series power decoupling capability for connecting PV to a single-phase power grid," in IET Power Electronics, vol. 10, no. 5, pp. 517-524, 21 4 2017.

[15] B. Pakkiraiah and G. Durga Sukumar, “Research Survey on Various MPPT Performance Issues to Improve the Solar PV System Efficiency”, in Journal of Solar Energy, vol. 2016, pp 1 – 20, 2016.

[16] Y. Liu, H. Wang, M. Huang, X. Zha and Y. Liu, "Influence of DC Link Capacitance on Power Efficiency of Single-Phase Inverter," 2018 IEEE Energy Conversion Congress and Exposition (ECCE), Portland, OR, pp. 1498-1504, 2018

[17] A. C. Kyritsis, E. C. Tatakis, N. P. Papanikolaou, “Optimum design of the current-source flyback inverter for decentralized grid-connected

photovoltaic systems" IEEE Transac. En. Convers. vol 23 no 1 pp 281–293, 2008

[18] G. Ertasgin, D. M. Whaley, N. Ertugrul, "Analysis and design of energy storage for current-source 1-ph grid-connected PV inverters" 23rd App. Pow. Elect. Conf. and Expo., APEC 2008) pp 1229–1234, February 2008

[19] T. F. Wu, C. H. Chang, Y. D. Chang, "Power loss analysis of grid connection photovoltaic system" Pow. Elect. and Drive Systems, PEDS, pp 326–331, November 2009

[20] M. Hanif, M. Basu, K. Gaughan, "Understanding the operation of Z-source inverter for photovoltaic application with a design example" IET Power Electron, vol 4 no 3 pp 278–287, 2011

[21] T. Shimizu, K. Wada, and N. Nakamura. "Flyback-Type Single-Phase Utility Interactive Inverter With Power Pulsation Decoupling on the DC Input for an AC Photovoltaic Module System". IEEE Transac. On Power Electro., Vol. 21, No. 5. pp: 1264 – 1272, 2006

[22] Y. Sun, Y. Liu, M. Su, W. Xiong and J. Yang, "Review of Active Power Decoupling Topologies in Single-Phase Systems," in IEEE Transactions on Power Electronics, vol. 31, no. 7, pp. 4778-4794, July 2016

[23] S. Zengin, F. Deveci, M. Boztepe. "Volt-second-based control method for discontinuous conduction mode flyback micro-inverters to improve total harmonic distortion" IET Pow. Elect. Vol. 6. No. 8. pp: 1600 –1607, 2013.

[24] H. Han, Y. Liu, Y. Sun, M. Su and W. Xiong, "Single-phase current source converter with power decoupling capability using a series-connected active buffer," in IET Power Electronics, vol. 8, no. 5, pp. 700-707, 5 2015.

[25] S. Kim, S. Lee, J. S. Lee and M. Kim, "Dual-mode flyback inverters in grid-connected photovoltaic systems," in IET Renewable Power Generation, vol. 10, no. 9, pp. 1402-1412, 10 2016.

[26] R. Za'im, J. Jamaludin and N. A. Rahim, "Photovoltaic Flyback Microinverter With Tertiary Winding Current Sensing," in IEEE Transactions on Power Electronics, vol. 34, no. 8, pp. 7588-7602, Aug. 2019.

[27] J. Kan, Y. Wu, Y. Tang and L. Jiang, "DLFCR Reduction Based on Power Predictive Scheme for Full-Bridge Photovoltaic Microinverter," in IEEE Transactions on Industrial Electronics, vol. 67, no. 6, pp. 4658-4669, June 2020.

[28] D. Wu, Y. Wu, J. Kan, Y. Tang, J. Chen and L. Jiang, "Full-Bridge Current-Fed PV Microinverter With DLFCR Reduction Ability," in IEEE Transactions on Power Electronics, vol. 35, no. 9, pp. 9543-9554, Sept. 2020.

[29] O. A. Montes, S. Son, J. Kim, J. S. Lee and M. Kim, "Duty-Ratio Feedforward Controller Design to Minimize the Capacitor Effect of the Flyback Inverter Under the Light-Load Condition," in IEEE Transactions on Power Electronics, vol. 33, no. 12, pp. 10979-10989, Dec. 2018.

[30] M. Kim, O. A. Montes, S. Son, Y. Choi and M. Kim, "Power Factor Improvement of Flyback PFC Converter Operating at the Light Load," 2019 IEEE Applied Power Electronics Conference and Exposition (APEC), Anaheim, CA, USA, pp. 3019-3023, 2019.

[31] J. Kan, Y. Wu, Y. Tang, S. Xie and L. Jiang, "Hybrid Control Scheme for Photovoltaic Microinverter With Adaptive Inductor," in IEEE Transactions on Power Electronics, vol. 34, no. 9, pp. 8762-8774, Sept. 2019.

[32] M. Karaca, A. Mamizadeh, N. Genc and A. Sular, "Analysis of Passive Filters for PV Inverters Under Variable Irradiances," 2019 8th International Conference on Renewable Energy Research and Applications (ICRERA), Brasov, Romania, pp. 680-685, 2019.

[33] S. Marhraoui, A. Abbou, N. El Hichami, S. E. Rhaili and M. R. Tur, "Grid-Connected PV Using Sliding Mode Based on Incremental Conductance MPPT and VSC," 2019 8th International Conference on Renewable Energy Research and Applications (ICRERA), Brasov, Romania, pp. 516-520, 2019.

[34] D. Gueye, A. Ndiaye, M. A. Tankari, M. Faye, A. Thiam, L. Thiaw, G. Lefebvre, "Design Methodology of Novel PID for Efficient Integration of PV Power to Electrical Distributed Network," in International Journal of Smart Grid, vol. 2, No. 1, pp. 78 – 86, 2018

[35] X. Li, H. Wen and Y. Hu, "Evaluation of different maximum power point tracking (MPPT) techniques based on practical meteorological data," 2016 IEEE International Conference on Renewable Energy Research and Applications (ICRERA), Birmingham, pp. 696-701, 2016.

[36] B. Veerasamy, A. R. Thelkar, G. Ramu and T. Takeshita, "Efficient MPPT control for fast irradiation changes and partial shading conditions on PV systems," 2016 IEEE International Conference on Renewable Energy Research and Applications (ICRERA), Birmingham, pp. 358-363, 2016.

[37] F. Ronilaya, I. Siradjuddin, S. E. Wibowo, I. Ridzki, "A new implementation of single phase Shimizu inverter for optimal power flow of solar PV system based on incremental conductance method", in ICIC Express Letter, vol.12, no. 7, pp 621 – 630, 2018.

[38] R.W Erickson, D. Maksimovic,: 2001. "Fundamentals of power electronics". Kluwer Academic Pub., Ch. 7

[39] M. Järvelä, K. Lappalainen, S. Valkealahti, "Characteristics of the cloud enhancement phenomenon and PV power plants", in Solar Energy, vol. 196, pp. 137 – 145, 2020